BULGARIAN ACADEMY OF SCIENCES

CYBERNETICS AND INFORMATION TECHNOLOGIES • Volume **24**, No 3
Sofia • 2024 Print ISSN: 1311-9702; Online ISSN: 1314-4081
DOI: 10.2478/cait-2024-0025

Advanced PSO Algorithms Development with Combined lbest and gbest Neighborhood Topologies

Romasevych Yuriy[1], *Loveikin Viatcheslav*[1], *Brand Ziv*[2]

[1]*Department of Machines and Equipment Design, National University of Life and Environmental Sciences of Ukraine, Kyiv, 03041, Ukraine*
[2]*The Control Research Center, Sami Shamoon College of Engineering, Be'er Sheva, 8410802, Israel*
E-mails: romasevichyuriy@ukr.net lovvs@ukr.net zivbr@sce.ac.il

***Abstract*:** *This paper introduces an innovative approach integrating global best* (*gbest*) *and local best* (*lbest*) *PSO communication topologies. The algorithm initiates with lbest and seamlessly transitions to gbest, with the switching rate controlled by the parameter "a". Rational values of "a" is determined through numerical experiments. A comparative methodology employing two estimation criteria is used to showcase the improved performance of the modified PSO-based algorithms. Furthermore, the efficacy of this approach is demonstrated in addressing two optimal control problems within dynamical systems. Results highlight the modified algorithms' superiority in terms of the total number of successful runs and statistical indicators. Consequently, these advanced algorithms prove effective for applications such as artificial neural network training, controller gains determination, and similar problem domains.*

***Keywords*:** *Particle swarm optimization, Topology connections, Benchmarks, Optimal control problems.*

1. Introduction

Optimization problems appear in many areas of human activity. From ancient ages to modern times this class of problems has experienced huge transformations. Problems became more complex and difficult to solve due to increased dimensionality, non-linearity, and constraints. Optimization methods have evolved as well. Now scholars focus on numerical approaches, as they can find appropriate solutions utilizing reasonable computational resources. One may hope for quantum computations, which can bring the methodology of solving optimization problems to a qualitatively new level. However, it is a far perspective, and researchers should improve the existing optimization paradigm.

One of the most powerful and applicable optimization algorithms is known as Particle Swarm Optimization (PSO) [1]. Since its development in

1995, it experienced a plethora of modifications, and the flow of academic papers in this direction is increasing year by year. Indeed, one might check the number of PSO-related works indexed in Scopus and Web of Science databases about the total works there (Fig. 1). All data presented in Fig. 1 were collected on the 9th of June 2023.

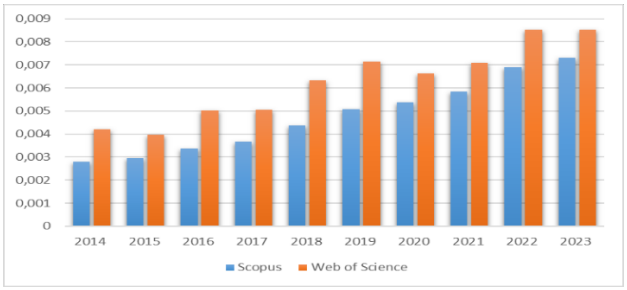

(a)

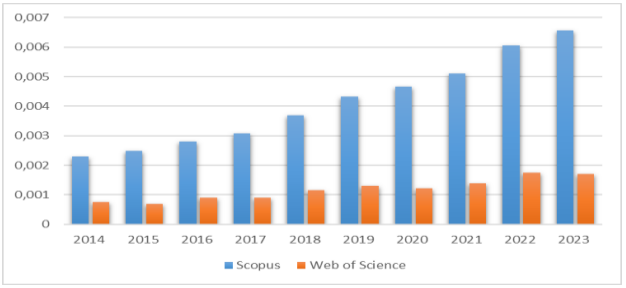

(b)

Fig. 1. Histograms of a fraction of PSO-related works indexed in Scopus and Web of Science databases corresponding to the total works there, which are collected by the requests: "PSO" (a); "PSO application" (b)

Histograms, shown in Fig. 1 clearly evidence, that the interest of the scientific community in PSO-connected investigations is increasing.

One of the features, that allows classifying PSO-related algorithms, is the level of connections between particles in a swarm: in gbest scheme, a particle "knows" about the best solution found by a whole swarm, in lbest, a particle obtains information only from a local neighborhood of particles [2, 3]. It, in turn, brings opposite search features. Gbest rapidly converges and may skip good solutions, lbest explores a cost function much more in detail but its convergence rate is low [3-5]. Other papers stress the similarity in the algorithms' search outputs [6]. Cited work, and some others [7, 8] put "vs" between gbest and lbest. In our opinion, this operator must be replaced with "and" one. An explanation of this idea is presented further.

The article is built in the following manner: the next section presents a brief review of the published works in the problem sphere; the third section describes the development of PSO modification where gbest and lbest are combined, in this section optimal value of additional algorithm parameter *a* is found; in the fourth section comparative analysis is shown on the set of well-known benchmarks; application of

developed algorithms to optimal control is discussed in the fifth section; the article ends with conclusions.

2. Literature review

Topology connections between particles in a swarm are an important feature that has a great impact on PSO Algorithm performance. In PSO-related reviews [3, 9-12] this factor is stressed. A huge number of studies reveal different aspects of topology connections swarm diversity and its changing during an algorithm execution [13, 14], probabilities features of particles' interactions [15], algorithm performance [4, 5, 8, 16, 17], etc. These works allowed understanding the features of gbest and lbest search patterns. The general point of the scholars' community is – overall gbest and lbest performances differ from each other [3-5]. However, the results of the investigation [6, 18, 19] refute this thesis. Engelbrecht [6] has performed a comparison of gbest and lbest PSO algorithms on 60 benchmarks constrained minimization problems of varying complexities have not been carried out. The statistical analysis shows that the two algorithms performed very similarly with respect to solution accuracy; gbest PSO performed slightly better with respect to success rate and efficiency; lbest PSO performed slightly better with respect to consistency. Thus, at least this contradiction must be properly studied.

To improve algorithm performance, a few studies have been conducted to combine gbest and lbest. For instance, article [20] describes a Unified PSO scheme (UPSO) – the algorithm, that harnesses the local and global search patterns. Their combination is carried out in a stochastic manner. Based on the application results, which involve five benchmarks, authors conclude, that UPSO exploits positive properties of both variants. Paper [21] has developed a new hybridized version of PSO with variable neighborhood search (PSOLGENT). It combines local and global expanding neighborhood topology by adding in velocity adaptation expression a fourth term. It directs a particle towards the local best of its neighborhood. PSOLGENT exploitation for constrained shortest path problems approved the efficiency of such an approach. In the study [22] All-Dimension-Neighborhood-based PSO with a randomly selected neighbors learning strategy (ADN-RSN-PSO) is developed. The idea of this algorithm is connected with a two-stage strategy: in the early iterations randomly selected neighbors learning strategy is adopted and it improves the swarm diversity, while in the later stage all-dimension neighborhood technique is used to accelerate the convergence rate. Experiments on CEC2013 benchmarks have shown algorithm competitiveness.

Different lbest topologies may be combined as well [23]. A good balance of exploitation and exploration activities, which is implemented in the so-called SMPSO-SW algorithm, is described in the work. The algorithm uses star topology during the first half of the iterations and the wheel topology during the second half. It has been applied to multi-objective optimization problems and revealed strong competitive features.

It is worth noting, also that in general, the topology concept may be used not only in PSO, but also in other agent-based optimization algorithms [24].

Summing everything up, we might conclude, that a combination of lbest and gbest features in one algorithm is an attractive direction of the investigation, which can bring promising results: good convergence rate, local minima avoiding, reasonable spending of computational budget, etc.

3. lbest and gbest fusion

3.1. Canonical PSO Algorithm, gbest and lbest

The canonical PSO Algorithm [1] operates with the term "swarm", it is a set of possible problem solutions (particles). A swarm may be imaged as a bunch of particles on a cost function surface. The number of particles – swarm population N, and a particle number denotes as n, $n \in [1, N]$. The position of a particle is described by a position vector $\mathrm{x}^n = [x_1^n, ..., x_d^n, ..., x_D^n]^{\mathrm{T}}$, a particle's direction of movement and velocity is described by a velocity vector

$$\mathrm{v}^n = [v_1^n, ..., v_d^n, ..., v_D^n]^{\mathrm{T}}, \tag{1}$$

where D signifies the dimension of particle n.

The PSO Algorithm starts with swarm design, which means random initialization of particles' positions and velocities. The velocity vector may be set as zero-vector (there are other possible techniques of velocity-vector initialization, but we will not consider them in the current investigation). Every component of the position vector of any particle is just a random number in the search domain, $x_d \in [x_{\min.d}, x_{\max.d}]$.

On the further algorithm's iterations velocity-vectors and position-vectors of particles are changed according to the equations:

$$\begin{cases} \mathrm{v}_j = \mathrm{w} \times \mathrm{v}_{j-1} + c_1 \mathrm{r}_1 \times (\mathrm{p}_{j-1} - \mathrm{x}_{j-1}) + c_2 \mathrm{r}_2 \times (\mathrm{g}_{j-1} - \mathrm{x}_{j-1}), \\ \mathrm{x}_j = \mathrm{x}_{j-1} + \mathrm{v}_j, \end{cases} \tag{2}$$

where: j is the number of the current iteration, $j \in [1, J]$, and J is the total number of iterations; p is particle's personal best – the best solution, which a particle has found so far; g is global best – the best solution, which the whole swarm has found; w is vector of weight coefficients; c_1 and c_2 are the cognitive and social coefficients; r_1 and r_2 are the vectors of random numbers, which uniformly generated on the interval [0, 1].

If the application of update rules (2) leads to the search domain leaving, then the corresponding component of the position vector must be replaced by the boundary value, which is violated ($x_{\min.d}$ or $x_{\max.d}$).

To update vectors p and g, the following formulas should be used:

$$\begin{cases} \mathrm{p}_{j.n} = \mathrm{x}_{j.n} \quad \text{if} \quad f(\mathrm{x}_{j.n}) < f(\mathrm{p}_{j.n}), \\ \mathrm{g}_{j.n} = \mathrm{p}_{j.n} \quad \text{if} \quad f(\mathrm{p}_{j.n}) < f(\mathrm{g}_{j.n}). \end{cases} \tag{3}$$

where f is a cost/objective function denotation.

The algorithm runs until the stopping criterion is met, most often $j=J$.

Social term in (2) severely influences particle movement. Indeed, every particle "knows" about vector g and is forced to go there. In many cases, it leads to premature

convergence, and problem solution remains unfound. Described topology connections between particles is known as gbest.

In order to avoid premature convergence, information about vector g must disseminate through a swarm at a much slower rate. One of the possible ways to reach this feature is to consider not a whole swarm, but a local neighborhood. This approach means, that in the first line of the system (2) the following expression should be used:

$$\mathrm{v}_j = \mathrm{w} \times \mathrm{v}_{j-1} + c_1 \mathrm{r}_1 \times (\mathrm{p}_{j-1} - \mathrm{x}_{j-1}) + c_2 \mathrm{r}_2 \times (\mathrm{gl}_{j-1} - \mathrm{x}_{j-1}), \tag{4}$$

where gl is the local best – the best solution, which a limited set (neighborhood) of particles has found. Application of expression (4) provides an exchange of information about found best solution only in the local group. On the next iterations, this information leaks to the next neighborhoods, since a particle belongs to different local groups. Described above scheme of information dissemination is called lbest.

We will show two possible structures of lbest: Ring [25] (very common; denoted as Ring-PSO) and rotation-Ring topologies [26] (denoted as R-Ring-PSO). The first means, that *n*-th particle exchanges information only with its left, (*n* – 1)-th, and right (*n*+1)-th neighbors, i.e., vector gl may be determined as follows:

$$\mathrm{gl}_{j.n} = \begin{cases} n = 1, \ \min\limits_{\arg}\left(f(\mathrm{p}_{j.N}), \ f(\mathrm{p}_{j.n}), \ f(\mathrm{p}_{j.n+1}) \right), \\ 2 \le n \le N-1, \ \min\limits_{\arg}\left(f(\mathrm{p}_{j.n-1}), \ f(\mathrm{p}_{j.n}), \ f(\mathrm{p}_{j.n+1}) \right), \\ n = N, \ \min\limits_{\arg}\left(f(\mathrm{p}_{j.n-1}), \ f(\mathrm{p}_{j.n}), \ f(\mathrm{p}_{j.1}) \right). \end{cases} \tag{5}$$

In the R-Ring-PSO neighborhood topology at each iteration, a particle changes its neighbors in a manner, that may be described by the idea of a rotation ring, i.e., the subscripts (sequence number) of left-side and right-side particles at each iteration are increased by one. After *N* iterations these subscripts return to values, they were on the first iteration. Thus, Ring-PSO exploits static topology, while R-Ring-PSO – dynamic one.

Both algorithms provide a detailed exploration of a cost function but suffer from a slow convergence [25, 26]. It, in turn, means a bigger amount of computational resources, which are necessary for finding a problem solution. The next subsection describes the approach to improve the situation.

3.2. Combination of lbest and gbest

Comparing both approaches gbest and lbest we may conclude, that lbest is good for the exploration phase, gbest – for exploitation. To combine their desired features, we propose to take into consideration a vector ggl, which must replace vector gl in the expression (4). To meet the search scheme "exploration-exploitation" vector ggl must be close to vector gl in the early phases of algorithm execution (lbest pattern), and close to vector g at the final phase of the search (gbest pattern). We propose to design a vector ggl component *d* with the following expression:

$$\mathrm{ggl}_{j.d} = \begin{cases} \left(\frac{j}{J}\right)^a \ge r, \ \mathrm{g}_{j.d}, \\ \left(\frac{j}{J}\right)^a < r, \ \mathrm{gl}_{j.d}, \end{cases} \tag{6}$$

where a is an algorithm new parameter, which controls the speed of patterns switching (from lbest to gbest); r is the random number, that is uniformly generated in the range [0, 1] with mathematical expectation $E(r)=0.5$. Its influence on developed algorithms performance will be given in further.

The manner of vector ggl design is similar to that, applied in the Differential Evolution (DE) Algorithm [27] for construction of the candidate solution (crossover).

In order to illustrate the influence of parameter a on the threshold value $(j/J)^a$, which switches components of vectors g and gl, plots (Fig. 2) are given.

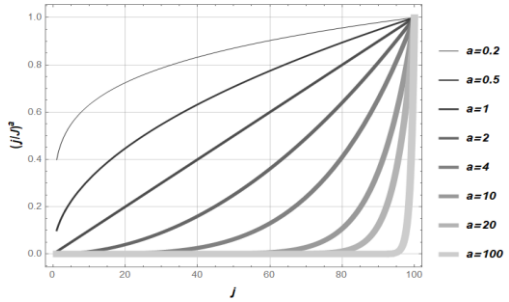

Fig. 2. Plots of influence of parameter a on the threshold value $(j/J)^a$

Mentioned above transition is carried out smoothly (Fig. 2), in a probable manner. From Fig. 2 one may observe, that for the case $a>1$ lbest pattern is prevailing, for $a<1$ gbest pattern has a bigger influence. Considering the fact, that $E(r)=0.5$, we may state an approximate estimation of the percentage of iterations, then the influence of the gbest pattern overpowers the lbest one (Table 1).

Table 1. Percentage of iterations, then the influence of the gbest pattern overpowers the lbest one

a value	0.2	0.5	1	2	4	10	20	100
Percentage of executed iterations	3	25	50	71	84	93	97	99

As one may conclude from the data given in Table 1, when $a\approx 0$, then the gbest pattern prevails, when $a>>1$, then the lbest pattern plays a principal role. In the boundary cases:

$$\begin{cases} \lim\limits_{a\to\infty} \mathrm{ggl} = \mathrm{gl}, \\ \lim\limits_{a\to 0} \mathrm{ggl} = \mathrm{g}. \end{cases} \tag{7}$$

Thus, gbest and lbest patterns are partial cases of the developed one.

For further investigations, we select static and dynamic ring topology of particles' connections. However, it may be applied to any algorithm in the lbest set. Developed algorithms is denoted as LG-Ring-PSO (parent algorithm is Ring-PSO) and LG-R-Ring-PSO (parent algorithm is R-Ring-PSO).

3.3. Set of benchmarks

To study the influence of a parameter on developed PSO modification and compare its performance with other PSO-based algorithms twenty benchmark functions are used [28-32].

3.4. Algorithms' optimal parameter determination

Many papers [9-11] argue the strong influence of parameters numerical values on PSO-based algorithms performance. Since parameter *a* governs switching between gbest and lbest, we should determine its reasonable value. In order to obtain it, a set of numerical experiments were carried out. In these experiments parameter *a* is just an independent argument of some function. The latter may be chosen as some statistical indicator of multiple LG-Ring-PSO and LG-R-Ring-PSO runs. We focus on the median value. For this purpose, it is very convenient to present Numerical Experiments Output (NEO) as a Box-Whisker diagrams in a logarithmic scale. All the data are collected on fifty independent algorithms runs. Benchmark's f1, f4, f7, and f8 were chosen for the estimation of parameter a influence. These functions were chosen since they have different features in terms of unimodality and separability.

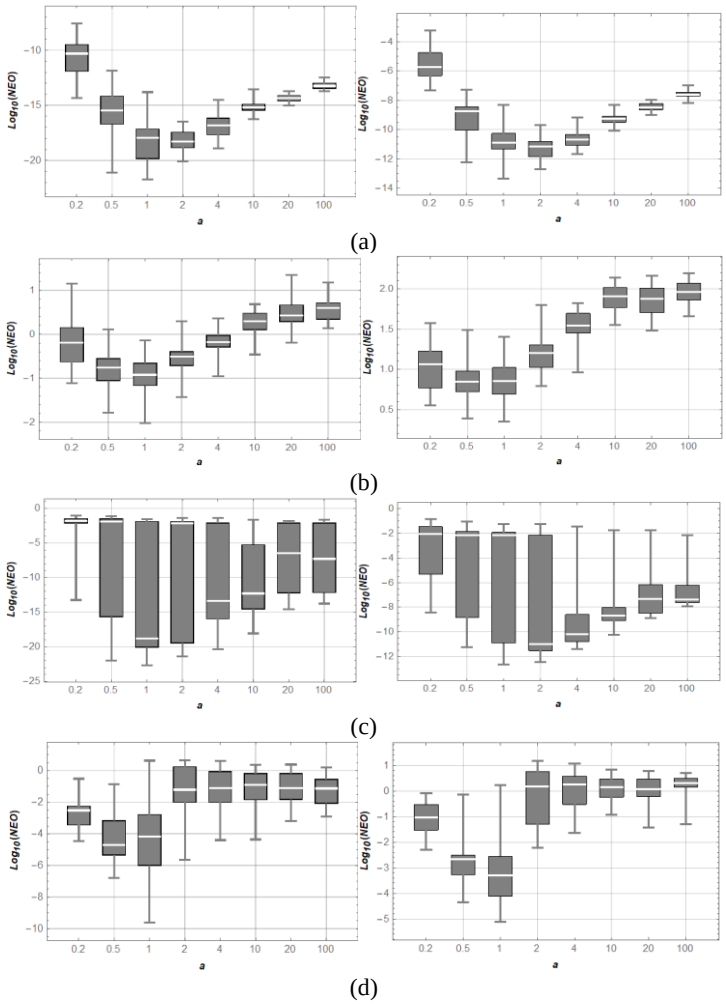

(a)

(b)

(c)

(d)

Fig. 3. Box-Whisker diagrams, which correspond to NEO of the algorithm LG-Ring-PSO referred to the benchmarks: f1 (a); f4 (b); f7 (c); f8 (d)

We set two cases: $D=N=30$ and $D=N=50$ (it is reasonable to apply developed algorithms to problems, where number of arguments do not exceed a hundred). Swarm population N should be increased for more complicated problems (in terms of value D). That is why for all of the considered cases $D=N$. In addition, two cases will bring more reliable data.

All the built diagrams are given in Fig. 3 where left column of diagrams refers to the case $D=N=30$, right one – to the case $D=N=50$. Analysis of plots (Fig. 3) allows us to determine a reasonable range of a values, which is associated with a median minimum (horizontal white lines on Fig. 3). For benchmarks f1, f4, and f7 it is located in domain [1, 2]. For benchmark f8 the domain of reasonable a values locates in [0.5, 1]. We recommend setting $a=1$ and will use it in further investigations.

Similar results were obtained for LG-Ring-R-PSO (Fig. 4). Here optimal a value for cases f1, f7, and f8 equals 4, for f4 one should set $a=0.5$. However, in further calculations, we set $a=4$.

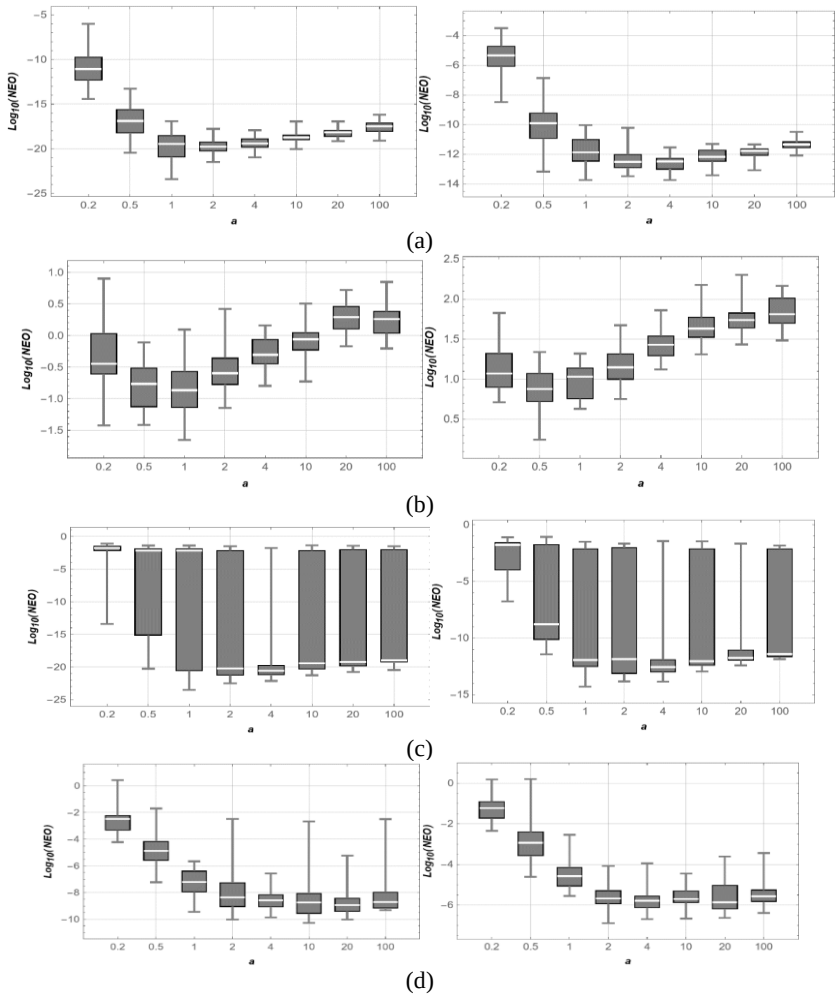

Fig. 4. Box-Whisker diagrams, which correspond to NEO of the algorithm LG-Ring-PSO referred to the benchmarks: f1 (a); f4 (b); f7 (c); f8 (d)

4. Comparative analysis

4.1. Estimation criteria

To estimate the algorithm's performance a set of criteria should be involved. "Raw" statistical values (minimax, maximal, average, median, standard deviation) are only source material for further estimations. They may be carried out on the base of the selected criteria.

One of the most common criteria of comparison is the sum of algorithms' ranks (noted as C1 in the paper). Algorithms ranking involves median value on fifty independent runs. This criterion allows in a quite simple manner to compare algorithms' performances (in a ranking sense) without concerning benchmarks minimization difficulties. To consider this, we propose to use a modification of a criterion, developed in [33]. The first step in criterion (noted as C2) calculation is Performance Matrix (PM) design. Every element of the matrix is calculated according to the following formula:

$$\mathrm{Cr}_{\beta.\alpha} = \log_{10}\left(\frac{S(f_{\beta.\alpha.j=1})}{S(f_{\beta.\alpha.j=J})}\right),\ \beta \in (1,...,B);\ \alpha \in (1,...,A), \tag{8}$$

where α and β are the compared algorithms and benchmarks counters respectively; A and B are the total numbers of compared algorithms and benchmarks respectively; S is the notation of some statistical value (for instance, median S=Me). Value (8) indicates by how many orders of magnitude algorithm α minimizes benchmark β during J iterations. PM contains this information through all algorithms and all benchmarks.

The only exclusion may trap, when during minimization a cost function changes its sign, i.e., logarithm function (8) is unidentified.

Since benchmarks differ from each other by the difficulty of minimum localization, the algorithms' performance must be weighted. For that purpose, we put into consideration a weight vector:

$$\begin{aligned} &\mathrm{Q} = (Q_1,..., Q_\beta,..., Q_B)^{\mathrm{T}}, \\ &\mathrm{Q}_\beta = A^{-1}\left\|\mathrm{Cr}_{\beta.\alpha}\right\|_L,\ \beta = \mathrm{const};\ \alpha \in (1,..., A), \end{aligned} \tag{9}$$

where $\left\|\mathrm{Cr}_{\beta.\alpha}\right\|_L$ is a norm of a vector, which corresponds to the β-th row of the PM. The next step is a calculation of the Weighted Performance Matrix (WPM). Each element of the WPM is obtained as follows:

$$\tilde{\mathrm{Cr}}_{\beta.\alpha} = \mathrm{Cr}_{\beta.\alpha} \times \mathrm{Q}_\beta^{-1}. \tag{10}$$

Value (10) reflects algorithm α performance with relation to the difficulty of benchmark β minimization. The last step is a calculation of the overall weighted algorithm performance. For that, all the elements (10) in the WPM columns must be added, $\mathrm{C2} = \sum_{\beta=1}^{B} \tilde{\mathrm{Cr}}_{\beta.\alpha}$.

In the case L=∞, we obtain a known criterion [33], which is very strong. In the paper, we will exploit L=2 variant (Euclidian norm). It is not so strict, as that applied

in the work [33], and allows to estimate algorithms' performances on a more reasonable basis.

4.2. Brief analysis

In this subsection, we present the data of eight optimization algorithms' performances. Algorithms belong to three sets: gbest, lbest, and gbest+lbest. They are LWD-PSO [34], VCT-PSO [35], ME-D-PSO [33], Ring-PSO [25], R-Ring-PSO [26], UPSO [20], LG-Ring-PSO, and LG-R-Ring-PSO. For all cases the number of iterations J=1000, swarm population N=50, and dimensionality of the benchmarks D=50. All the obtained "raw" data are given in [36. Table 1].

The smallest values of statistical indicators in Table B.1 are given in bold. Based on median values (most uninfluenced by the stochastic factor of the algorithms search) we provided a ranking of the algorithms' performances (criterion C1). The corresponding data are given in [36, Table 2].

Another indicator – is C2, which is calculated on the median base as well. To calculate C2 values, WPM was found (exception cases are f3, f17, and f19; for these, it is impossible to calculate $Cr_{\beta.\alpha}$). WPM is presented in [36, Table 3].

Both tables (Table 2 and Table 3 in [36]) evidence, that the proposed approach of gbest and lbest combination beneficially influences their search performance. Indeed, found with LG-Ring-PSO and LG-R-Ring-PSO solutions are greatly better, than, those, determined with parent algorithms (Ring-PSO and R-Ring-PSO). For LG-R-Ring-PSO Algorithm modification (6) allowed improvement of search performance for all benchmarks, except f16 and f20. Overall C1 increasing equals 30 points (approximately 33% of initial performance). Similar numbers for LG-Ring-PSO are 11 points of C1 increase (10% of initial performance). Relative increasing of C2 indicator for LG-R-Ring-PSO is 15%, for LG-Ring-PSO – 6%. Thus, modification (6) influences better on more advanced PSO-based algorithms.

Among compared algorithms the best search abilities (estimated by criteria C1 and C2) shows LG-R-Ring-PSO. It outperforms the nearest algorithm (UPSO). However, we cannot recommend LG-R-Ring-PSO for wide application so far. The reason is connected with the fact, that solved optimization problems (f1-f20) are synthetic. They reflect features of real-world optimization problems only to some extent. That is why estimation and comparison of algorithms' performances is mandatory for further LG-R-Ring-PSO and LG-Ring-PSO competitive ability justification.

5. Application to Optimal Control Problems (OCP)

5.1. Solution of OCP-1

In this subsection we state and solve an optimal control problem [34]. The plant to control – is an underactuated non-linear pendular system – Furuta pendulum [37, 38] (Fig. 5).

This dynamical system is described by the following system of non-linear differential equations:

$$(11)\qquad \begin{cases} \ddot{\alpha}(J_0 + J_{21}\sin^2(\phi)) + \ddot{\phi}m_2L_1l_2\cos(\phi) - m_2L_1l_2\sin(\phi)\dot{\phi}^2 + \dot{\alpha}\dot{\phi}J_{21}\sin(2\phi) = \mathrm{M}, \\ \ddot{\alpha}m_2L_1l_2\cos(\phi) + \ddot{\phi}J_{21} - \frac{1}{2}\dot{\phi}^2J_{21}\sin(2\phi) + gm_2l_2\sin(\phi) = 0. \end{cases}$$

Here ϕ and α are the generalized coordinates of the system; M is the drive torque; L_1 and L_2 are the lengths of Arm 1 which rotates in the horizontal plane and Arm 2 which is free to rotate in the vertical plane; the arms possess masses denoted as m_1 and m_2, with corresponding distances from the pivot point to their respective centers of mass referred to as l_1 and l_2; J_0 denotes the total moment of inertia experienced by the motor rotor when the pendulum (Arm 2) is in its stable equilibrium position, hanging vertically downward, $J_0 = J_1 + m_1l_1^2 + m_2L_1^2$; J_1 is the moment of inertia of Arm 1 about the pivot point; J_{21} is the total moment of inertia of Arm 2 about its pivot point, $J_{21} = J_2 + m_2l_2^2$; J_2 is the moment of inertia of Arm 2 about the free point; g is gravitational acceleration. Numerical parameters of the system are listed below: L_1=2.78×10^{-1} m, L_2=3.0×10^{-1} m, l_1=1.5×10^{-1} m, l_2=1.48×10^{-1} m, m_1=3.0×10^{-1} kg, m_2=7.5×10^{-2} kg, J_1=2.48×10^{-2} kg.m^2, J_2=3.86×10^{-3} kg.m^2.

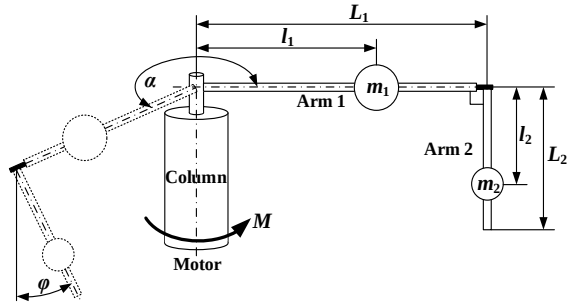

Fig. 5. Dynamical model of Furuta pendulum

Boundary conditions of the controlled movement are as follows:

$$(12)\qquad \begin{cases} \phi(0) = \pi;\ \dot{\phi}(0) = \alpha(0) = \dot{\alpha}(0) = 0, \\ |\phi(t_s)| < \phi_a;\ |\dot{\phi}(t_s)| < \dot{\phi}_a;\ |\alpha(t_s)| < \alpha_a;\ |\dot{\alpha}(t_s)| < \dot{\alpha}_a, \end{cases}$$

where t_s is settling time (to determine its value the simulation of the dynamical system movement must be ceased when all the final conditions (10) are met and t_s is set as the moment of simulation termination); ϕ_a and α_a are the acceptable value of final generalized coordinates (ϕ_a=α_a=10^{-2} rad); $\dot{\phi}_a$ and $\dot{\alpha}_a$ are the acceptable value of final generalized angular velocities ($\dot{\phi}_a$ = $\dot{\alpha}_a$ =10^{-2} rad/s). Because of the limitation of a torque M, caused by technical features of a drive, the following constraints must be taken into consideration:

$$(13)\qquad \mathrm{M}_{min} \le \mathrm{M} \le \mathrm{M}_{max},$$

where M_{min} and M_{max} – minimal and maximal torques, which can be applied to the column (M_{max}=1 N.m, M_{min}= –1 N.m). In order to satisfy conditions (13) output signal of the control operator, which will be described further, is passed through the saturation element. It cuts the values of torque M, that violate constrain (13).

A Criterion Cr to be minimized includes four components:

$$\text{Cr} = 2\pi\Omega t_s + M_{\max}^{-1}\sqrt{t_s^{-1}\int_0^{t_s} M^2 dt} + \pi^{-1}\sqrt{t_s^{-1}\int_0^{t_s} \alpha^2 dt} + \pi^{-1}\sqrt{t_s^{-1}\int_0^{t_s} \phi^2 dt}, \tag{14}$$

where Ω is the frequency of natural system oscillations, $\Omega = \sqrt{\frac{J_1}{g l_2 m_2}}$. The first term in (14) corresponds to the system's movement duration, the second term – to the control resources, spent on the system movement (also this term can be presented as energy losses in the motor), the third and fourth components relate to the minimization of generalized coordinates deviation from final conditions (12). All the terms of criterion (14) are dimensionless and they reflect the undesirable features of the system controlled movement. That is why Cr must be minimized.

Since optimal control problem (11)-(14) is nonlinear, it is reasonable to use a nonlinear control operator to find its solution [37]. In the investigation, we apply a feedforward Artificial Neural Network (ANN) with one hidden layer. Indeed, ANN may form a nonlinear mapping of the input vector (state variables) to the output function (control). We may expect this mapping to meet all the problem conditions (11)-(14).

Optimization algorithms, studied in this work, will be used to find the parameters of ANN, since the problem (11)-(14) solving directly is impossible: algorithms find optimal values of arguments, but in the stated problem we need to find optimal mapping "state variables – optimal control". That is why we exploit the ANN, it includes parameters to find (PSO algorithms will find them) and builds the needed mapping.

ANN has four inputs (generalized coordinates and velocities) and one output – torque M. The hidden layer includes five artificial neurons. Arctg – is an artificial neuron's activation function. Thus, the problem (11)-(14) is reduced to the finding of thirty-one parameters of ANN (twenty-five weights and six biases). Such parameters must define the ANN behavior (control), that allows to satisfy boundary conditions (11) and minimize criterion (14) (reinforcement training paradigm). The search domain of each ANN parameter is limited by the range [–2, 2].

In the ANN training, we consider two stages. The first one is associated with conditions (12) satisfaction, i.e., following terminal criterion must be minimized:

$$\text{Ter} = \begin{cases} \delta_T\left(|\phi(t_s)|\phi_a^{-1} + |\dot{\phi}(t_s)|\dot{\phi}_a^{-1} + |\alpha(t_s)|\alpha_a^{-1} + |\dot{\alpha}(t_s)|\dot{\alpha}_a^{-1}\right) \text{ if} \\ |\phi(t_s)| > \phi_a \vee |\dot{\phi}(t_s)| > \dot{\phi}_a \vee |\alpha(t_s)| > \alpha_a \vee |\dot{\alpha}(t_s)| > \dot{\alpha}_a, \\ 0 \text{ if } |\phi(t_s)| \le \phi_a \wedge |\dot{\phi}(t_s)| \le \dot{\phi}_a \wedge |\alpha(t_s)| \le \alpha_a \wedge |\dot{\alpha}(t_s)| \le \dot{\alpha}_a. \end{cases} \tag{15}$$

where δ_T – Terminal weight coefficient (δ_T=10^5), it allows to separate the stage of Ter minimization from the stage of Cr minimization.

The second stage is pure minimization of criterion (14), without *Ter* (15). At the beginning of the second stage, gbest includes ANN parameters, which allow ANN to act in a manner, that satisfies final conditions (12).

For all cases, the number of iterations J=200, swarm population N=30, and there were fifty of each (compared) algorithm runs. The result of criterion minimization in ANN reinforcement training for the best found solution are given in Fig. 6.

One can observe both described stages in Fig. 6, a (a sharp decrease of Cr+Ter value). Phase trajectories of Furuta pendulum links support the fact of final conditions (12) satisfaction. However, fast torque M changing in some periods is an undesirable feature of the found control, and that is why there is room for further system dynamics improvement.

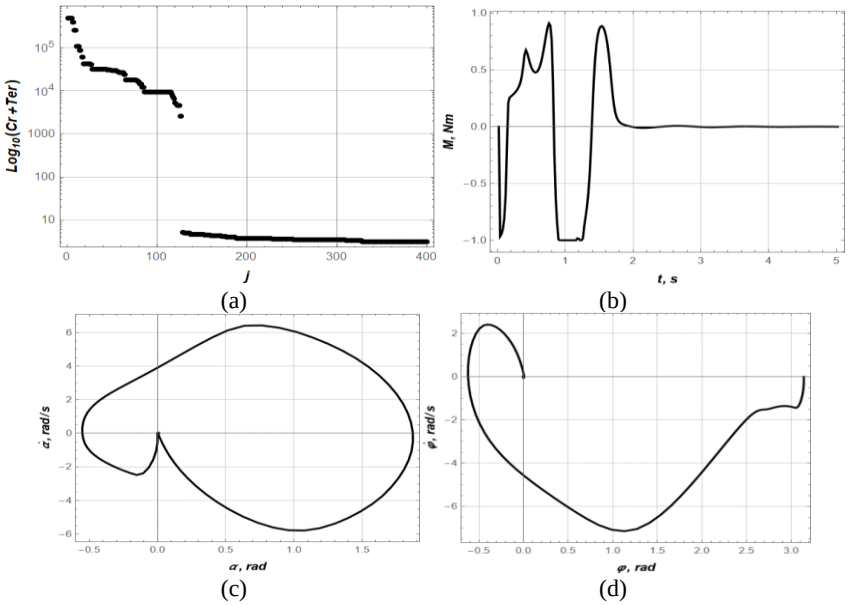

(a) (b) (c) (d)

Fig. 6. Results of optimal control problem solution: decreasing of Cr (a); torque M (b); phase trajectory of the boom (c); phase trajectory of the pendulum link (d)

Summing everything up, we may state, that LG-Ring-PSO and LG-R-Ring-PSO are perspective algorithms for ANN training, particularly in the reinforcement paradigm [40].

5.2. Solution of OCP-2

The cantilever beam is a widely recognized and prominent case study, spanning diverse research fields from aerospace to land-based and maritime applications. This case study has become a crucial testbed within the control systems domain, showcasing innovative advancements in vibration suppression through closed-loop control systems. Researchers have addressed various control aspects, exploring algorithmic developments, optimization methodologies for sensor and actuator placement, and the meticulous selection of sensor and actuator types [41-43]. In a notable study by H u a n g et al. [41], they successfully integrated a global canonical Particle Swarm Optimization (PSO) algorithm to optimize an LQR cost function for vibration mitigation in a cantilever beam. Utilizing an actuator and a piezoelectric sensor, this approach demonstrated remarkable efficacy in suppressing vibrations, as evidenced by simulation results.

The following section presents comparative results of various PSO approaches, including those proposed in this paper, for mitigating vibrations in a cantilever beam.

The analysis focuses on a cantilever beam featuring a bending Moment actuator (M) and an external Force (F) applied near the clamping and at the end of the beam, as illustrated in Fig. 7.

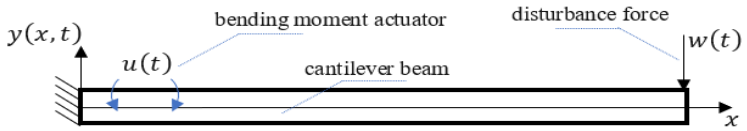

Fig. 7. Smart cantilever beam with piezoelectric patches

The cantilever beam model is a continuous system described by a partial differential equation based on the Euler-Bernoulli beam theory. The model is as follows:

$$\sqrt{\frac{EI}{\rho w}}\frac{\partial^4 y(x,t)}{\partial x^4}+\frac{\partial^2 y(x,t)}{\partial t^4}=w(t)+u(t). \tag{16}$$

This model can be represented in finite dimensions using equations of motion in modal space as follows:

$$\mathrm{M}\times\ddot{\mathrm{g}}(t)+\mathrm{C}\times\dot{\mathrm{g}}(t)+\mathrm{K}\times\mathrm{g}(t)=\mathrm{F}(t). \tag{17}$$

In that equation, $\mathrm{M}\in\mathbb{R}^{m\times m}$, $\mathrm{C}\in\mathbb{R}^{m\times m}$ and $\mathrm{K}\in\mathbb{R}^{m\times m}$ represent the modal mass matrix, damping matrix, and stiffness matrix of the beam, respectively; F corresponds to the modal load matrix, generated by the bending moment actuator (u) and the disturbance force (w); $\mathrm{g}\in\mathbb{R}^{m}$ represents the modal coordinate, where m is the number of modes.

The piezoelectric actuator forms the control action, causing the suppression of beam vibrations, while the piezoelectric sensor provides actual information about the current system state. In this case, the equations of motion (17) can be rewritten in a state-space model as

$$\begin{cases}\dot{\mathrm{x}}(t)=\mathrm{A}\times\mathrm{x}(t)+\mathrm{B}\times\mathrm{u}(t)+\mathrm{E}\times\mathrm{w}(t),\\ \mathrm{y}(t)=\mathrm{C}\times\mathrm{x}(t),\\ \mathrm{x}(0)=\mathrm{x}_0,\end{cases} \tag{18}$$

where: x is the state vector; x_0 is the initial state vector (zero-vector); y is the output vector, and C is the output matrix, defined by the sensor's type, sensitivity, and location.

For the PSO investigation, a model with two first modes (m=2) were chosen. The relationship can be expressed as follows:

$$\mathrm{A}=\begin{pmatrix}0 & 0 & 1 & 0\\ 0 & 0 & 0 & 1\\ -1.23\times10^{-10} & 0 & -5.13 & 0\\ 0 & -3.27\times10^{3} & 0 & -8.28\times10^{-1}\end{pmatrix}, \tag{19}$$

$$\mathrm{B}=(0,\,0,\,2.68\times10^{3},\,-1.95\times10^{2})^{\mathrm{T}},$$

$$\mathrm{C}=(4.90\times10^{-1},\,-2.14\times10^{-1},\,0,\,0),$$

$$\mathrm{E}=(0,\,0,\,5,\,5)^{\mathrm{T}}.$$

The disturbance input, denoted as w, is designed to consist of two impacts of opposite signs.

(20)
$$w=\begin{cases}1, & 0\le t\le 0.1,\\ -1, & 0.1<t\le 0.2,\\ 0, & 0.2<t.\end{cases}$$

We define the class of admissible control laws, denoted as u, to be of the form:

(21)
$$u=G_1x_1+G_2x_2+G_3\dot{x}_1+G_4\dot{x}_2,$$

where G_1, …, G_4 are the controller gains to be defined to satisfy final conditions,

(22)
$$|x(t_s)|<|x_a(t_s)|,$$

and complex criterion minimization,

(23)
$$Cr=\sqrt{t_s^{-1}\int_0^{t_s}(x_1x_2)^2+(\dot{x}_1\dot{x}_2)^2dt}+$$
$$+\max(|u|)+0.5(\max(|x_1|)+\max(|x_2|)+\max(|\dot{x}_1|)+\max(|\dot{x}_2|)).$$

Finally, the admissible state vector is set as follows: $x_a(t_s)$ = (5×10^{-7}, 5×10^{-7}, 5×10^{-7}, 5×10^{-7})^T. To satisfy all the conditions (22) and (23) we applied a similar technique – splitting the solution into two stages. In the first, an algorithm finds a solution, which meets final conditions (22), while in the second one, criterion (23) is minimized. In OCP-2 we set $\delta_T=10^{10}$ since the values of state-vector components are quite small. The search domain of controller gains G_1, G_2, G_3, G_4 is limited by the range [–0.5, 0.5]. Since the total number of the controller gains is four, we set J=50, and N=10. Each algorithm was run fifty times. The result of criterion minimization for the best found solution is given in Fig. 8a.

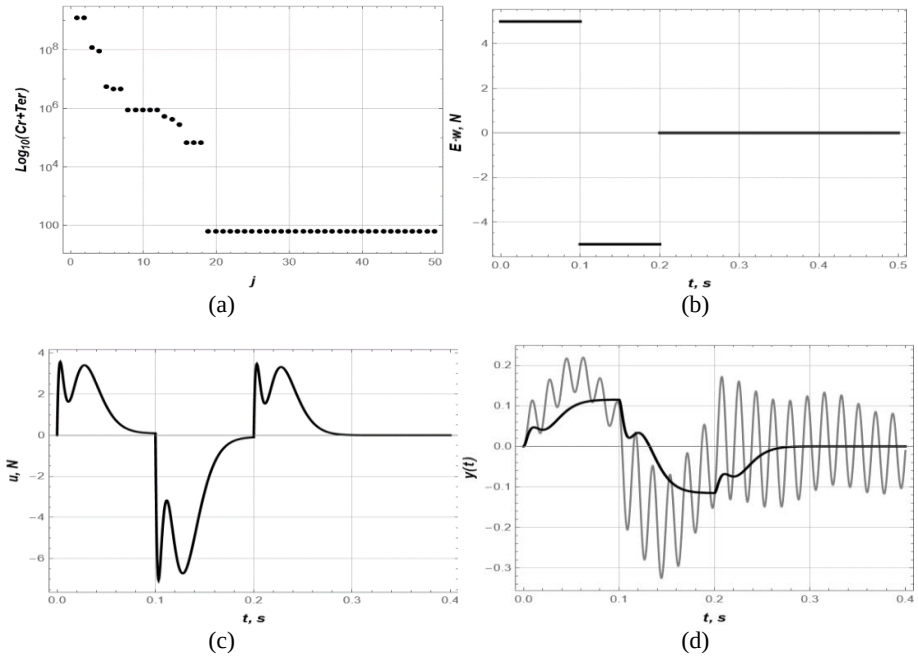

(a) (b) (c) (d)

Fig. 8. Results of optimal control problem solution: decreasing of Cr+Ter (a); disturbance function (b); control function (c); systems response (gray curve – without control; black curve – with optimal control) (d)

OCP-2 problem is much simpler than OCP-1, and the optimization algorithm needs only eighteen iterations (Fig. 8a) to find a solution, which satisfies conditions (22). Vibration of the beam, caused by disturbance (Fig. 8b) is suppressed (Fig. 8d). Thus, we may recommend LG-Ring-PSO and LG-R-Ring-PSO algorithms for application in similar problems.

Overall optimization algorithms performance on OCP-1 and OCP-2 is given in Table 4 in [36]. Analysis of the data in this table shows that LG-Ring-PSO and LG-R-Ring-PSO outperform compared algorithms. The initial modification, R-Ring-PSO, is very close, but almost all statistical values related to LG-R-Ring-PSO are better. Thus, we strongly recommend using the LG-R-Ring-PSO Algorithm, especially for applications to OCPs.

6. Conclusions

The article proposes an approach to enhance the search capabilities of PSO-based algorithms, combining lbest and gbest topologies for particle connections. This fusion is tailored to address the "exploration-exploitation" balance in algorithm activity: lbest prevails in the early stages of the search, while gbest dominates towards the end. The transition between them is controlled by an additional algorithm parameter, denoted as a, whose optimal value is determined in this paper. However, certain exceptions noted in the study suggest a more general case: a should be individually selected for each function to be minimized before the algorithm starts or adaptively during its execution. This presents an area for further investigation.

Numerical experiments involving twenty benchmarks were conducted to validate the enhancements introduced in the modified algorithms (Ring-PSO and R-Ring-PSO). The results were analyzed, and two evaluation criteria were calculated for each of the eight compared optimization algorithms, confirming the superiority of LG-Ring-PSO and LG-R-Ring-PSO. Furthermore, the eight compared optimization algorithms were applied to two nonlinear OCPs, intentionally chosen for their differences in control operator, constraints, criterion for minimization, and time constants. The results of the OCP solutions demonstrated the high efficiency of LG-Ring-PSO and LG-R-Ring-PSO algorithms.

Future directions in this research branch, in addition to those already mentioned, involve exploring other lbest topology algorithms, studying their convergence behaviour, testing algorithms on a broader set of benchmarks, and applying them to more complex optimization problems.

***Acknowledgments*:** The article is prepared as a part of the joint Ukrainian-Israeli R&D Project „Development of new modifications of PSO method and their application in engineering problems" (Research supported by Ministry of Innovation, Science & Technology, Israel, Grant 0005185 and Ministry of Education & Science of Ukraine, Ukraine, Grant M/67-2023).

References

1. Kennedy, J., R. C. Eberhart. Particle Swarm Optimization. – In: Proc. of IEEE International Conference on Neural Networks, 1995, pp. 1942-1948.
2. Houssein, E. H., A. G. Gad, K. Hussain, P. N. Suganthan. Major Advances in Particle Swarm Optimization: Theory, Analysis, and Application. – Swarm and Evolutionary Computation, Vol. **63**, 2021, 100868. DOI: 10.1016/j.swevo.2021.100868.
3. Freitas, D., L. G. Lopes, F. Morgado-Dias. Particle Swarm Optimisation: A Historical Review Up to the Current Developments. – Entropy, Vol. **22**, 2020, No 3, 362. DOI: 10.3390/e22030362.
4. Blackwell, T., J. Kennedy. Impact of Communication Topology in Particle Swarm Optimization. – IEEE Transactions on Evolutionary Computation, Vol. **23**, 2019, No 4, pp. 689-702. DOI: 10.1109/tevc.2018.2880894.
5. Kennedy, J., R. Mendes (n.d.). Population Structure and Particle Swarm Performance. – In: Proc. of Congress on Evolutionary Computation (CEC'02), 2002 (Cat. No 02TH8600). DOI: 10.1109/cec.2002.1004493.
6. Engelbrecht, A. P. Particle Swarm Optimization: Global Best or Local Best? – In: Proc. of BRICS Congress on Computational Intelligence and 11th Brazilian Congress on Computational Intelligence, 2013. DOI: 10.1109/brics-cci-cbic.2013.31.
7. Liu, H., B. Li, Y. Ji, T. Sun (n.d.). Particle Swarm Optimisation from lbest to gbest. – Applied Soft Computing Technologies: The Challenge of Complexity, pp. 537-545. DOI: 10.1007/3-540-31662-0_41.
8. Vazquez, J. C., F. Valdez, P. Melin. Comparative Study of Social Network Structures in PSO. – Recent Advances on Hybrid Approaches for Designing Intelligent Systems, 2014, pp. 239-254. DOI: 10.1007/978-3-319-05170-3_17.
9. Ahmed, G. G. Particle Swarm Optimization Algorithm and Its Applications: A Systematic Review. – Archives of Computational Methods in Engineering, Vol. **29**, 2022, pp. 2531-2561. DOI: 10.1007/s11831-021-09694-4.
10. Shami, T. M., A. A. El-Saleh, M. Alswaitti, Q. Al-Tashi, M. A. Summakieh, S. Mirjalili. Particle Swarm Optimization: A Comprehensive Survey. – IEEE Access, Vol. **10**, 2022, pp. 10031-10061. DOI: 10.1109/ACCESS.2022.3142859
11. Houssein, E. H., A. G. Gad, K. Hussain, P. N. Suganthan. Major Advances in Particle Swarm Optimization: Theory, Analysis, and Application. – Swarm and Evolutionary Computation, Vol. **63**, 2021, 100868. DOI: 10.1016/j.swevo.2021.100868.
12. Yudong, Z., W. Shuihua, J. Genlin. A Comprehensive Survey on Particle Swarm Optimization. Algorithm and Its Applications. – Mathematical Problems in Engineering, Vol. **38**, 2015, 931256. DOI: org/10.1155/2015/931256.
13. Pluhacek, M., A. Kazikova, T. Kadavy, A. Viktorin, R. Senkerik. Relation of Neighborhood Size and Diversity Loss Rate in Particle Swarm Optimization with Ring Topology. Mendel. – Soft Computing Journal, Vol. **27**, 2021, No 2, pp. 74-79. DOI: 10.13164/mendel.2021.k.0d9.
14. Ni, J. C., L. Li, F. Qiao. A Topology Based on a Local World Evolving Model for PSO. – Advanced Materials Research, Vol. **219-220**, 2011, pp. 1297-1300. DOI: 10.4028/www.scientific.net/amr.219-220.1297.
15. Ghosh, S., D. Kundu, K. Suresh, S. Das, A. Abraham, B. K. Panigrahi, V. Snasel. On Some Properties of the lbest Topology in Particle Swarm Optimization. – In: Proc. of 9th International Conference on Hybrid Intelligent Systems, 2009. DOI: 10.1109/his.2009.288.
16. Fernandes, C. M., A. C. Rosa, J. L. J. Laredo, C. Cotta, J. J. Merelo. A Study on Time-Varying Partially Connected Topologies for the Particle Swarm. – In: Proc. of IEEE Congress on Evolutionary Computation, 2013. DOI: 10.1109/cec.2013.6557863.
17. Tsujimoto, T., T. Shindo, T. Kimura, K. Jin'no. A Relationship between Network Topology and Search Performance of PSO. – In: Proc. of IEEE Congress on Evolutionary Computation. 2,012. DOI: 10.1109/cec.2012.6256536.

18. S u g a n t h a n, P. N. Particle Swarm Optimiser with Neighbourhood Operator. – In: Proc. of Congress on Evolutionary Computation-CEC99 (Cat. No 99TH8406), Washington, DC, USA, Vol. **3**, 1999, pp. 1958-1962. DOI: 10.1109/CEC.1999.785514.
19. K e n n e d y, J. Stereotyping: Improving Particle Swarm Performance with Cluster Analysis. – In: Proc. of Congress on Evolutionary Computation. CEC00 (Cat. No 00TH8512), La Jolla, CA, USA, Vol. **2**, 2000, pp. 1507-1512. DOI: 10.1109/CEC.2000.870832.
20. P a r s o p o u l u s, K. E., N. M. V r a h a t i s. UPSO: A Unified Particle Swarm Optimization Scheme. – Lecture Series on Computational Siences, 2004, No 1, pp. 868-873.
21. M a r i n a k i s, Y., A. M i g d a l a s, A. S i f a l e r a s. A Hybrid Particle Swarm Optimization – Variable Neighborhood Search Algorithm for Constrained Shortest Path Problems. – European Journal of Operational Research, Vol. **261**, 2017, No 3, pp. 819-834. DOI: 10.1016/j.ejor.2017.03.031.
22. W e i, S., L. A n p i n g, Y. H o n g s h a n, L. Q i a o k a n g, W. G u o h u a. All-Dimension Neighborhood Based Particle Swarm Optimization with Randomly Selected Neighbors. – Information Sciences, 2017, pp. 1-22. DOI: 10.1016/j.ins.2017.04.007.
23. H. Ishibuchi, Q. Zhang, R. Cheng, K. Li, H. Li, H. Wang, A. Zhou, Eds. Evolutionary Multi-Criterion Optimization. – In: Lecture Notes in Computer Science. 2021. DOI:10.1007/978-3-030-72062-9.
24. L y n n, N., M. Z. A l i, P. N. S u g a n t h a n. Population Topologies for Particle Swarm Optimization and Differential Evolution. – Swarm and Evolutionary Computation, Vol. **39**, 2018, pp. 24-35. DOI: 10.1016/j.swevo.2017.11.002.
25. L i, X. Niching without Niching Parameters: Particle Swarm Optimization Using a Ring Topology. – IEEE Transactions on Evolutionary Computation, Vol. **14**, 2010, No 1, pp. 150-169, 5352335. DOI: 10.1109/TEVC.2009.2026270.
26. R o m a s e v y c h, Y., V. L o v e i k i n, Y. L o v e i k i n. Development of New Rotating Ring Topology of PSO-Algorithm. – In: Proc. of 2nd IEEE KhPI Week on Advanced Technology (KhPIWeek'21), Kharkiv, Ukraine, 2021, pp. 79-82. DOI: 10.1109/KhPIWeek53812.2021.9569973.
27. S t o r n, R., K. P r i c e. Differential Evolution – A Simple and Efficient Heuristic for Global Optimization Over Continuous Spaces. – Journal of Global Optimization, Vol. **11**, 1997, No 4, pp. 341-359.
28. Optimization & Eye Pleasure: 78 Benchmark Test Functions for Single Objective Optimization. **https://towardsdatascience.com/optimization-eye-pleasure-78-benchmark-test-functions-for-single-objective-optimization-92e7ed1d1f12**
29. Virtual Library of Simulation Experiments: Test Functions and Datasets. Optimization Test Problems. **https://www.sfu.ca/~ssurjano/optimization.html**
30. HappyCat – A Simple Function Class Where Well-Known Direct Search Algorithms Do Fail. **https://homepages.fhv.at/hgb/New-Papers/PPSN12_BF12.pdf**
31. M o m i n, J., Y. X i n-S h e. A Literature Survey of Benchmark Functions for Global Optimization Problems. – Int. Journal of Mathematical Modelling and Numerical Optimisation, Vol. **4**, 2013, No 2, pp. 150-194. DOI: 10.1504/IJMMNO.2013.055204.
32. M o n t a z, A. M., C. K h o m p a t r a p o r n, Z. B. Z a b i n s k y. A Numerical Evaluation of Several Stochastic Algorithms on Selected Continuous Global Optimization Test Problems. – Journal of Global Optimization, Vol. **31**, 2005, pp. 635-672. DOI: 10.1007/s10898-004-9972-2.
33. R o m a s e v y c h, Y., V. L o v e i k i n, V. M a k a r e t s. Optimal Constrained Tuning of PI-Controllers via a New PSO-Based Technique. – International Journal of Swarm Intelligence Research, Vol. **11**, 2020, No 4, pp. 87-105. DOI: 10.4018/IJSIR.2020100104.
34. S h i, Y., R. E b e r h a r t. A Modified Particle Swarm Optimizer. – In: Proc. of IEEE International Conference on Evolutionary Computation Proceedings. IEEE World Congress on Computational Intelligence, 1998, pp. 69-73. DOI: 10.1109/ICEC.1998.699146.
35. R o m a s e v y c h, Y., V. L o v e i k i n, Y. L o v e i k i n. Development of a PSO Modification with Varying Cognitive Term. – In: Proc. of 3rd IEEE KhPI Week on Advanced Technology (KhPIWeek), IEEE, 2022, pp. 55-59. DOI: 10.1109/KhPIWeek57572.2022.9916413.

36. Article Additional Data.
https://drive.google.com/file/d/1Oj5-GzgcztnCWHDRYazkIhjvTkpHTzW8/view?usp=sharing
37. Romasevych, Y., V. Loveikin, M. Ohiienko, L. Shymko, K. Łukawiecki. Innovation Management in Agriculture. Agrotronics and Design of Optimal Controllers Based on New Modifications of Particle Swarm Optimization, 2021.
https://www.wszia.opole.pl/wp-content/uploads/2020/09/Mon_Romasevich.pdf
38. Cazzolato, B. S., Z. Prime. On the Dynamics of the Furuta Pendulum. – Journal of Control Science and Engineering, 2011, Article ID 528341. 8 p. DOI: 10.1155/2011/528341.
39. Antonio-Cruz, M., V. M. Hernandez-Guzman, C. A. Merlo-Zapata, C. Marquez-Sanchez. Nonlinear Control with Friction Compensation to Swing-Up a Furuta Pendulum. – ISA Transactions, Vol. **139**, 2023, pp. 713-723. DOI: 10.1016/j.isatra.2023.05.007.
40. Dallali, H., P. Kormushev, Z. Li, D. Caldwell. On Global Optimization of Walking Gaits for the Compliant Humanoid Robot, COMAN Using Reinforcement Learning. – Cybernetics and Information Technologies, Vol. **12**, 2012, No 3, pp. 39-52.
41. Huang, Z., F. Huang, X. Wang, F. Chu. Active Vibration Control of Composite Cantilever Beams. – Materials, Vol. **16**, 2023, 95. DOI: 10.3390/ma16010095.
42. Huang, Z., Y. Mao, A. Dai, M. Han, X. Wang, F. Chu. Active Vibration Control of Piezoelectric Sandwich Plates. – Materials, Vol. **15**, 2022, 3907. DOI: 10.3390/ma15113907.
43. Xin, Z., D. Gao, S. Lu, X. Fu, Y. Zhu, J. Xu. Research of Active Vibration Control for Cantilever Beam Based on Macro Fiber Composite Actuators. – In: Proc. of International Conference on Cyber-Physical Social Intelligence (ICCSI'22), Nanjing, China, 2022, pp. 573-577. DOI: 10.1109/ICCSI55536.2022.9970636.

Received: 06.12.2023; Second Version: 14.07.2024; Accepted: 12.08.2024